The viscous stress in a non-homogeneous suspension

Kengo Ichiki[1, 2, *] and Andrea Prosperetti[1, 2, †]

[1]*Department of Mechanical Engineering, The Johns Hopkins University, Baltimore MD 21218*
[2]*Faculty of Applied Physics, Twente Institute of Mechanics, and Burgerscentrum, University of Twente, AE 7500 Enschede, The Netherlands*

(Dated: July 7, 2004)

It has recently been shown that the average stress in a viscous suspension consists of a symmetric traceless component, and an antisymmetric component expressed in terms of a polar and an axial vector. In this paper, closure relations for these quantities are derived by means of numerical ensemble averaging following a systematic procedure. By the use of a suitably biased probability distribution, the ensemble is made to describe a spatially non-uniform system. Several new terms, which are identically zero for a homogeneous system, are identified.

I. INTRODUCTION

The central problem in the modeling of disperse multiphase flows by means of averaged equations is the closure of the terms which arise from the averaging procedure applied to the exact microscopic equations (see e.g. Refs. 1–4). Such closure requires that part of the information lost upon averaging be reintroduced to a degree of approximation sufficient to capture the physics and result in a well-posed mathematical model.

The problem has been recognized for a long time and many attempts at its solution can be found in the literature. A representative list may include the early paper by Anderson and Jackson[5] dealing with the formulation of a closed model for fluidized beds, the more recent work on the same topic described by Sundaresan[6], work by Koch, Sangani and collaborators devoted to gas-solid suspensions and bubbly liquids (see e.g. Refs. 7–11), the studies by Brady and co-workers on suspension rheology (see e.g. Refs. 12,14–16), and many others. While the ultimate goal of a general model capable of describing a variety of flow situations is still distant, considerable progress has been achieved by coupling analysis with the detailed computational simulation of flows with suspended particles. With few exceptions (see e.g. Refs. 17,18), most of the work has focused on the limit cases of potential flow (see e.g. Refs. 19–22) and Stokes flow (see e.g. Refs. 23–26), which seem to be the most amenable to the development of a closed model. While idealized, there is hope that the insight gained on these systems might shed useful light for the solution of the problem at intermediate Reynolds numbers.

In some recent papers[27–30] we have considered this problem, again in the Stokes flow limit, pointing out that the information obtainable from the simulation of spatially uniform systems can reflect only partially the full structure of the averaged equations. For example, in a uniform sheared suspension, on average the particles move with the same velocity as the mixture, which does not permit to see the effect of any closure term proportional to the average relative velocity of the two. Similarly, it is impossible to test the applicability of an effective viscosity calculated from the shear problem to a different flow situation, such as sedimentation, if spatial uniformity causes all spatial gradients to vanish.

To be sure, different flows give rise to different microstructures, which will then have an impact on the effective properties and closure relations (see e.g. Ref. 13,14). For this reason, the pursuit of a single closed system of averaged equations applicable to many different flow situations may be to some extent futile if a high degree of fidelity is pursued. However, one may look at the general class of problems from another angle. The development of closure relations which, while perhaps not exactly valid for any flow, still manage to capture in some generic sense several important features of many flows, might be a perhaps less ambitious but ultimately, in practice, more fruitful goal.

It is such a goal which we pursue in this paper: we use spatially periodic ensembles of hard spheres in a cubic fundamental cell to derive closure relations for suspensions of equal spheres in Stokes flow. A distinct feature of our approach is the ability to build into this ensemble (by post-processing, as it were) a prescribed spatial non-uniformity in the particle number density distribution.[30,31] In this way, we are able to discern at least some of the effects of non-uniformity alluded to before. One major such effect is the appearance of an antisymmetric component of the stress tensor, entirely due to spatial non-uniformity, even in the absence of couples acting on the particles.

A large fraction of the contemporary work on suspension theory has focused on non-Newtonian rheological properties (see e.g. Refs. 15,32). A great deal of attention has been paid to the anisotropy of the pair distribution function, assuming a spatially homogeneous particle number density. In the present paper we adopt a complementary viewpoint, focusing on non-uniformities of the particle number density while disregarding the anisotropy of the pair distribution function. We believe that our techniques can be extended to deal with the complete problem in which both the particle number density is non-uniform and pair distribution function anisotropic.

The logic to be followed in our study is straightforward in principle. We start by choosing the fundamental vari-

ables of the theory as the volume fraction, mixture velocity, relative particle-mixture (or "slip") velocity and relative particle-mixture angular velocity. Considerations of Galilean invariance, parity, linearity, and equipresence dictate the most general form relating the quantity to be closed – e.g., the stress – to quantities derived from the fundamental variables of the theory – e.g., the rate of strain of the mixture velocity. In general, the closure relation consists of a linear combination of such quantities the coefficients of which – e.g. the effective viscosity – depend on the volume fraction. At this point, the quantity to be closed is calculated directly from its definition by means of numerical ensemble averaging for some prescribed flows, and so are the other quantities appearing in the closure. Matching the two sides of the closure relation determines then the unknown volume-fraction-dependent coefficients. In this work, we use three different physical situations: an equal force applied to each particle, an equal torque applied to each particles, and a uniform shear imposed on the suspension.

Results of a nature similar to the present ones were presented earlier in Refs. 27 and 28. With respect to that work, the results of the present paper have the advantage of being based on the substantially improved theoretical framework developed in Ref. 33 (see e.g the comments at the end of section IV), of being numerically much more accurate thanks to a significantly increased number of simulations, and of covering a much greater number of particle volume fractions.

II. THE PARTICLE STRESS

We will use as our starting point an expression for the particle stress developed in Ref. 33. That work considered a system of N equal spheres suspended in a fluid occupying a cubic domain subjected to periodicity boundary conditions. A closed form expression was obtained for the mean mixture volumetric flux $\boldsymbol{u}_m$ and mixture pressure p_m in terms of ensemble averages of multipole coefficients appearing in Lamb's general solution for the Stokes flow past a sphere.[34–36] The situation considered was general and, in particular, did not assume a spatial homogeneity of the ensemble used to calculate the average. Upon calculating the gradient of p_m and the Laplacian of $\boldsymbol{u}_m$, the following result was found (Eq. (10.3) of Ref. 33):

$$-\boldsymbol{\nabla} p_m + \mu \nabla^2 \boldsymbol{u}_m \;=\; -\mu \left[\boldsymbol{\nabla} \cdot \mathsf{S} + \boldsymbol{\nabla} \times (\boldsymbol{R} - \boldsymbol{\nabla} \times \boldsymbol{V}) \right] + \frac{1}{v} \int_{|\boldsymbol{r}| \le a} d^3 r \, n(\boldsymbol{x}+\boldsymbol{r}) \, \overline{\boldsymbol{F}}(\boldsymbol{x}+\boldsymbol{r}) \quad (1)$$

Here S is a traceless symmetric two-tensor, $\boldsymbol{R}$ an axial vector, $\boldsymbol{V}$ a polar vector, n the particle number density, and $\overline{\boldsymbol{F}}$ the average force exerted by the fluid on the particles, each one with radius a and volume $v = \frac{4}{3}\pi a^3$. For a pure fluid with viscosity μ, the right-hand side of this equation would vanish (provided the body force is conservative and absorbed in the pressure p_m). The terms in the right-hand side must therefore be identified with the effect of the particles on the momentum balance of the mixture. If we combine the term containing $\boldsymbol{u}_m$ with the remaining terms, we find the divergence of a stress

$$\frac{1}{\mu} \boldsymbol{\Sigma} = 2\mathsf{E}_m + \mathsf{S} + \boldsymbol{\epsilon} \cdot (\boldsymbol{R} - \boldsymbol{\nabla} \times \boldsymbol{V}) \;, \quad (2)$$

in which $\boldsymbol{\epsilon}$ is the alternating tensor and

$$\mathsf{E}_m = \frac{1}{2} \left[\boldsymbol{\nabla} \boldsymbol{u}_m + (\boldsymbol{\nabla} \boldsymbol{u}_m)^\dagger \right] \;, \quad (3)$$

is the mixture rate-of-strain tensor. This expression explicitly shows that the stress tensor contains two antisymmetric contributions. It is possible to show that, for a uniform suspension,[13,37]

$$\boldsymbol{R} \;=\; -\frac{1}{2\mu} \, n \, \overline{\oint_{|\boldsymbol{r}|=a} dS \, \boldsymbol{r} \times [\boldsymbol{\sigma} \cdot \boldsymbol{n}]} \quad (4)$$

where the overline denotes the ensemble average, $\boldsymbol{\sigma}$ is the fluid stress, and $\boldsymbol{n}$ the outwardly directed unit normal at the particle surface. For couple-free particles in Stokes flow, this term will therefore vanish. However, as shown in section IV below, in the case of spatial non-uniformities, the expression of $\boldsymbol{R}$ contains additional terms that do not vanish even in the case of couple-free particles.

In the uniform case, it can be shown that the new term $\boldsymbol{V}$ is given by[37]

$$\boldsymbol{V} \;=\; \frac{1}{\mu} \, n \, \overline{\oint_{|\boldsymbol{r}|=a} dS \; (\mathsf{I} - \boldsymbol{n}\boldsymbol{n}) \cdot [\boldsymbol{\sigma} \cdot \boldsymbol{n}]} \,, \quad (5)$$

in which I is the identity two-tensor, and is therefore proportional to the surface-average tangential traction on the particle surface.

As shown in Ref. 33 and summarized in the Appendix, the exact expressions of S, $\boldsymbol{R}$, and $\boldsymbol{V}$ involve an infinite series of multipole coefficients, which reflect the finite size of the particles and therefore, ultimately, the non-local nature of an exact theory. The expressions (4) and (5) are the first terms of the respective infinite series. In this paper we will limit our consideration to the next few terms, which embody a low-order non-local correction. We may also note that, to first order in the particle volume fraction, it is possible to show that

$$\mathsf{S} = 5\phi \mathsf{E}_m \quad (6)$$

with the particle volume fraction given by

$$\phi(\boldsymbol{x}) \;=\; \int_{|\boldsymbol{r}| \le a} d^3 r \, n(\boldsymbol{x}+\boldsymbol{r}) \quad (7)$$

so that one recovers the well-known Einstein viscosity correction,[38] and that

$$\boldsymbol{R} = 3\phi \boldsymbol{\Omega}_\Delta, \quad (8)$$

$$\boldsymbol{V} = \frac{3}{10}\phi\ \boldsymbol{u}_\Delta + \frac{1}{7}a^2 \mathsf{E}_m \cdot \boldsymbol{\nabla}\phi - \frac{11}{140}\phi a^2 \nabla^2 \boldsymbol{u}_m, \qquad (9)$$

where $\boldsymbol{u}_\Delta = \boldsymbol{U} - \boldsymbol{u}_m$ is the slip translational velocity, defined by the difference between the volumetric flux $\boldsymbol{u}_m$ and the average particle translational velocity $\boldsymbol{U}$, and $\boldsymbol{\Omega}_\Delta = \boldsymbol{\Omega} - (1/2)\boldsymbol{\nabla} \times \boldsymbol{u}_m$ the slip angular velocity. The goal of this paper is to extend these dilute-limit results to the case of finite volume fraction by carrying out numerical ensemble averages.

III. THE SYMMETRIC PART OF THE STRESS

We assume that the contributions to the stress can be expressed in terms of the local particle volume fraction ϕ, mixture velocity $\boldsymbol{u}_m$, the average inter-phase (or slip) velocity $\boldsymbol{u}_\Delta$, and the average inter-phase angular velocity $\boldsymbol{\Omega}_\Delta$. Since S is a symmetric traceless tensor, if such a representation is possible, it must have the form

$$2\mathsf{E}_m + \mathsf{S} = 2\mu_e \mathsf{E}_m + \ldots \qquad (10)$$

in which μ_e is the usual effective viscosity normalized by the viscosity of the suspending fluid, and the dots stand for additional terms as explained in the Appendix A 2.

number of particles N_p	number of configurations N_c
10 – 16	2048
17 – 79	1024
80 – 150	512
160	256

TABLE I: Number of configurations in the ensemble used in the simulations for particle volume fractions between 1% and 40%.

We now apply to the present closure problem the same techniques developed earlier in Refs. 27,28,30. The method is described in detail in these references and in Ref. 30 and a brief summary will be sufficient here. We construct a homogeneous ensemble of hard-sphere configurations by placing N particles in a cubic box of side L and subjecting them to random displacements. For each value of the volume fraction, we construct in this way several ensembles containing between 10 and 160 spheres, and between 256 and 2048 configurations (see Table I and Ref. 30 for further details). For the intermediate volume fraction of 35% and particle numbers 62 and 80 we have found that the running average of most quantities settles within a band of less than 10% percent after about 700 configurations, and convergence improves as the number of particles increases. As explained later, due to the several ways in which the forcings can be chosen for each configuration, all the averages that are used in this work (except one) correspond as a minimum to three times the number of configurations shown in Table I.

While a direct averaging would produce ensemble averages corresponding to a spatially homogeneous system, by suitably biasing the uniform-system probability, we produce results which correspond to a non-uniform number density distribution

$$n(\boldsymbol{x}) = n_0 \left(1 + \epsilon \sin \boldsymbol{k} \cdot \boldsymbol{x}\right) \qquad (11)$$

in which $n_0 = N/L^3$, $\boldsymbol{k}$ is a vector with modulus $2\pi/L$ parallel to one of the sides of the box, and ϵ a small parameter. As a result of this procedure, to first order in ϵ, all the average quantities will consist of a constant part and a sinusoidal (or co-sinusoidal) disturbance. The introduction of the parameter ϵ enables us to identify unequivocally the latter part above the statistical noise. The use of ensembles with a different number of particles for the same volume fraction enables us to vary the box side L and, therefore, $\boldsymbol{k}$.

For each one of the flows considered here (applied force, index F; applied torque, index T, applied strain, index E), the symmetric stress S can be calculated directly from the results of the numerical simulations using its expression (A1) in terms of multipole coefficients, and the results suitably parameterized. For example, for the shear problem, we write

$$\begin{aligned} \mathsf{S}(\boldsymbol{x}) &= [S]^0_E \mathsf{E}^\infty \qquad (12) \\ &+ \epsilon \sin\left(\boldsymbol{k}\cdot\boldsymbol{x}\right)\left([S]^E_E \mathsf{E}^\infty + [S]^\perp_E \mathsf{G}^\perp_E + [S]^\parallel_E \mathsf{G}^\parallel_E\right), \end{aligned}$$

where $[S]^0_E$, $[S]^E_E$, $[S]^\perp_E$, and $[S]^\parallel_E$ are coefficients dependent on both the wave vector k and the volume fraction ϕ, E^∞ is the imposed rate of shear,

$$\mathsf{G}^\perp_E = \boldsymbol{W}^\perp_E \hat{\boldsymbol{k}} + \hat{\boldsymbol{k}} \boldsymbol{W}^\perp_E, \qquad (13)$$

$$\mathsf{G}^\parallel_E = \frac{1}{2}\left(\boldsymbol{W}^\parallel_E \hat{\boldsymbol{k}} + \hat{\boldsymbol{k}} \boldsymbol{W}^\parallel_E\right) - \frac{1}{3}\left(\hat{\boldsymbol{k}} \cdot \boldsymbol{W}^\parallel_E\right)\mathsf{I}, \qquad (14)$$

and

$$\boldsymbol{W}^\parallel_E = a\left(\hat{\boldsymbol{k}}\hat{\boldsymbol{k}}\right) \cdot \left(\mathsf{E}^\infty \cdot \hat{\boldsymbol{k}}\right), \qquad (15)$$

$$\boldsymbol{W}^\perp_E = a\left(\mathsf{I} - \hat{\boldsymbol{k}}\hat{\boldsymbol{k}}\right) \cdot \left(\mathsf{E}^\infty \cdot \hat{\boldsymbol{k}}\right). \qquad (16)$$

The numerical results for the mixture velocity are parameterized as

$$\boldsymbol{u}_m(\boldsymbol{x}) = \mathsf{E}^\infty \cdot \boldsymbol{x} + \epsilon \cos\left(\boldsymbol{k}\cdot\boldsymbol{x}\right)[u_m]^\perp_E \boldsymbol{W}^\perp_E, \qquad (17)$$

where $[u_m]^\perp_E$ is the numerically computed coefficient. Since E^∞ is symmetric and traceless and the problem linear, an arbitrary state of uniform shear can be represented by the linear combination of 5 linearly independent tensors. In our simulations, each configuration is subjected to each one of these base imposed shears, which has the effect of increasing the number of configurations by a factor of 2 for $[S]^\parallel_E$ and by a factor of 3 for the other parameters.

The parameterization (17) does not contain a term proportional to $\boldsymbol{W}^\parallel_E$ due to incompressibility, nor an analogous sine term as the corresponding coefficient is found

numerically to be many orders of magnitude smaller than $[u_m]^\perp_E$ and can therefore be assumed to vanish. By substituting this expression for $\boldsymbol{u}_m$ into (3), we find

$$\mathsf{E}_m \;=\; \mathsf{E}^\infty - \epsilon \sin\left(\boldsymbol{k}\cdot\boldsymbol{x}\right) \frac{k}{2}\,[u_m]^\perp_E\,\mathsf{G}^\perp_E. \tag{18}$$

Expressions analogous to (12) and (17) are found for the other average and closure quantities for each one of the three flows. The expressions for the force problem contain vectors $\boldsymbol{W}_F$, (defined later in Eq. 33) and those for the torque problem vectors $\boldsymbol{W}_T$ (defined in Eq. 60) which characterize each problem just as the two vectors $\boldsymbol{W}^\parallel_E$ and $\boldsymbol{W}^\perp_E$ are characteristic of the shear problem.

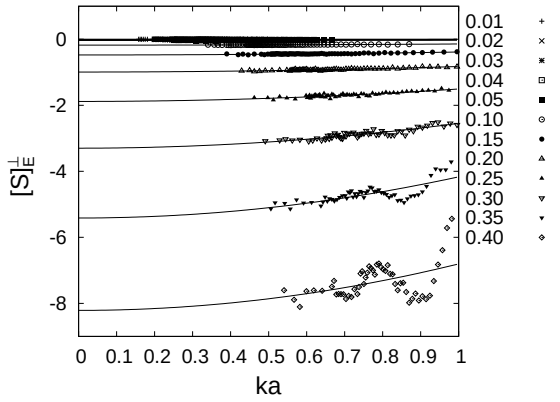

FIG. 1: An example of the k-dependence of the average coefficients appearing in Eq. (12) for $[S]^\perp_E$. This is the same coefficient shown in Fig. 1 of Ref. 28. Other examples can be found in Ref. 30.

An example of the k-dependence of one of the coefficients of S, $[S]^\perp_E$, is shown in Fig. 1. The results corresponding to each volume fraction are generated by carrying out simulations with a variable number of particles N in the fundamental cell according to the relation $ka = \left(6\pi^2\phi/N\right)^{1/3}$. At the higher volume fractions, this figure exhibits oscillations the origin of which is unclear. However, what is used for the present purposes is only the extrapolated limit to $ka = 0$, and the amplitude of the oscillations decreases for small k. In view of this fact and of the consistency observed in the results (discussed below), we believe that the truncation of the multipole expansions used in the simulation is adequate for the present purposes.

The numerical results are fitted as[30]

$$[S]^0_E \;=\; D^{[S]^0_E}, \tag{19}$$

$$[S]^E_E \;=\; D^{[S]^E_E} + (ka)^2 A^{[S]^E_E}, \tag{20}$$

$$[S]^\parallel_E \;=\; 0 + (ka)^2 A^{[S]^\parallel_E}, \tag{21}$$

$$[S]^\perp_E \;=\; D^{[S]^\perp_E} + (ka)^2 A^{[S]^\perp_E}. \tag{22}$$

The results for the other flows are fitted in the same way as shown in the Appendix A 2. Similar fits are generated for the k-dependence of the coefficients of $\boldsymbol{u}_m$ and of the other average quantities; for example

$$[u_m]^\perp_E \;=\; \frac{1}{k} D^{[u_m]^\perp_E} + k A^{[u_m]^\perp_E}. \tag{23}$$

Upon substituting the parameterizations (19) to (23) into the closure relation (10), equating corresponding terms, and taking the limit $k \to 0$ corresponding to an infinite system size, we find

$$\mu_e \;=\; 1 + \frac{1}{2} D^{[S]^0_E}, \tag{24}$$

$$\mu_e \;=\; 1 - \frac{D^{[S]^\perp_E}}{D^{[u_m]^\perp_E}}, \tag{25}$$

$$\frac{\mathrm{d}\mu_e}{\mathrm{d}\phi} \;=\; \frac{1}{2\phi} D^{[S]^E_E}. \tag{26}$$

The last relation is found recalling that $\mu_e = \mu_e(\phi)$ so that, if $\phi' = \phi(1 + \epsilon \sin \boldsymbol{k}\cdot\boldsymbol{x})$,

$$\mu_e(\phi') = \mu_e(\phi') + (\phi' - \phi)\,\frac{\mathrm{d}\mu_e}{\mathrm{d}\phi}. \tag{27}$$

The relations shown are derived from the leading powers of k in the parameterizations. In principle, additional relations could be found from the higher order terms. However, as we have shown in an earlier paper,[30] these higher-order terms appear to be affected by the finite size of the system simulated and therefore they would not lead to relations corresponding to intrinsic properties of the suspension.

By proceeding in th same fashion for the other problems – applied force and torque – one finds the analogous relations

$$\mu_e \;=\; 1 - \frac{D^{[S]^\perp_T}}{D^{[u_m]^\perp_T}}, \tag{28}$$

$$\mu_e \;=\; 1 + \frac{D^{[S]^\perp_F}}{D^{[u_m]^\perp_F}}. \tag{29}$$

It should be stressed that only the relation (24) for the effective viscosity can be derived by a consideration of a spatially homogeneous suspension. For example, in a uniformly sedimenting suspension, there would be no shear and, therefore, the terms containing μ_e would vanish identically. By considering the non-uniform case, we are now in a position to investigate whether the same μ_e which accounts for the effective viscosity of a sheared uniform suspension can account for the stress in a non-uniform suspension subjected to other forcings. In other words, consistency among the various expressions shown above would imply that μ_e is a robust quantity which has the same value in (at least) three very different physical situations. This issue addresses the question of the *very existence* of effective properties, in the sense of intrinsic descriptors of the suspension behavior in different flow situations.

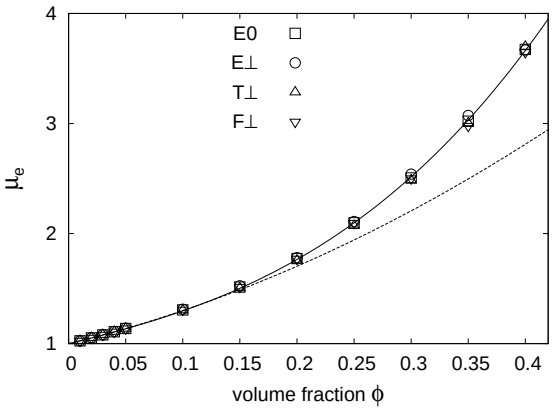

FIG. 2: μ_e from (24), (25), (28) and (29). Dashed and solid lines show the dilute-limit fit (30) and the whole-range fit $(5/2)\phi + A\phi^2 + B\phi^3$.

An excellent consistency can indeed be observed in Fig. 2, which shows μ_e calculated from the uniform part of the shear problem (open squares, Eq. 24), and from the non-uniform parts of the shear problem (open circles, Eq. 25), of the torque problem (up-triangles, Eq. 28), and of the force problem (down-triangles, Eq. 29).

A further consistency test is offered by comparing Eq. (26) for $d\mu_e/d\phi$ with the derivative calculated from the fitting as $\mathrm{d}\mu_e/\mathrm{d}\phi = 2.5 + 2A\phi + 3B\phi^2$ shown in Fig. 3. The observed consistency implies that, for weak spatial non-uniformity (as measured by ϵ, cf. Eq. 11), the effective viscosity only depends on the local value of the volume fraction.

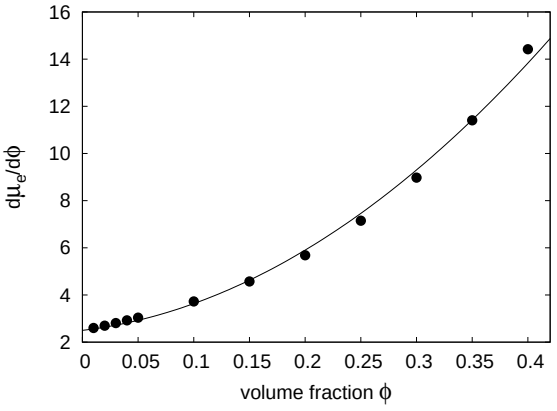

FIG. 3: $\mathrm{d}\mu_e/\mathrm{d}\phi$ from (26). The solid line is the derivative of the whole-range fit of μ_e given in the text.

For $\phi \leq 0.05$, our μ_e is well fitted by

$$\mu_e \;=\; 1 + \frac{5}{2}\phi + 5.07\phi^2. \qquad (30)$$

As mentioned before, the present calculations are done with the assumption of an isotropic two-body correlation function including multipoles up to the fifth order. It is well known that the coefficient of the ϕ^2 term depends on the multipole truncation,[39] as well as the microstructure, such as the anisotropy of the pair distribution function.[40] Our result 5.07 for this coefficient is consistent with earlier studies, such as 5.2 by Batchelor and Green[41] with all moments, and 4.84 by Beenakker[39] obtained by means of a concentration expansion. Over the whole range of ϕ, our numerical result for μ_e is well fitted by

$$\mu_e = 1 + 2.5\phi + A\phi^2 + B\phi^3\,, \qquad (31)$$

with $A = 2.84$ and $B = 18.9$ as shown by the solid line in Fig. 2.

Since in our calculation we only include multipoles up to the fifth order without lubrication corrections, the accuracy of our results decreases with increasing ϕ. For example, for $\phi = 25\%$ and 40%, we find $\mu_e = 2.10$ and 3.67, respectively, as shown in Table II, to be compared with 2.17 and 4.27 as reported by Ladd.[42]

TABLE II: Effective viscosity μ_e as computed for the shear of a uniform (E^0) and non-uniform ($E^\perp$) suspension, and for the flow induced by an applied torque ($T^\perp$) and force ($F^\perp$) to the particles of a non-uniform suspension.

ϕ	E^0	$E^\perp$	$T^\perp$	$F^\perp$
0.01	1.02548	1.025	1.025	1.0257
0.02	1.05196	1.051	1.052	1.0522
0.03	1.07947	1.079	1.080	1.0796
0.04	1.10810	1.108	1.109	1.1078
0.05	1.13788	1.138	1.137	1.1371
0.10	1.3063	1.312	1.305	1.300
0.15	1.5145	1.53	1.505	1.496
0.20	1.773	1.79	1.76	1.742
0.25	2.098	2.12	2.07	2.05
0.30	2.505	2.52	2.47	2.44
0.35	3.021	3.0	3.0	2.94
0.40	3.673	3.7	3.7	3.55

IV. THE POLAR VECTOR OF THE ANTISYMMETRIC STRESS

We proceed in the same way for the polar vector of the antisymmetric stress, $\boldsymbol{V}$. By including all the terms with the correct parity and vectorial nature which contribute to leading order in k we write

$$\begin{aligned}\boldsymbol{V} \;=\; & V_1\boldsymbol{u}_\Delta \\ & + V_2 a^2 \mathsf{E}_m \cdot \boldsymbol{\nabla}\phi + V_3 a^2 \nabla^2 \boldsymbol{u}_m \\ & + V_4 a^2 \boldsymbol{\nabla}\times\boldsymbol{\Omega}_\Delta + V_5 a^2\,(\boldsymbol{\nabla}\phi)\times\boldsymbol{\Omega}_\Delta, \end{aligned} \qquad (32)$$

where $\boldsymbol{\Omega}_\Delta$ is the angular "slip" velocity defined earlier after Eq. (9). It will be appreciated that the first term of $\boldsymbol{V}$ does not contain factors of the particle radius and, therefore, would not vanish in the limit $a/L \to 0$.

In this case, we discuss the parameterizations with reference to the force problem (index F), characterized by the vector

$$\boldsymbol{W}_F \;=\; \frac{\boldsymbol{F}_0}{6\pi\mu a} \tag{33}$$

which is the sedimentation velocity of a single isolated particle subjected to the force $\boldsymbol{F}_0$; the vectors $\boldsymbol{W}_F^{\parallel}$ and $\boldsymbol{W}_F^{\perp}$ are its projection parallel and orthogonal to the non-uniformity vector $\boldsymbol{k}$. By choosing, for each configuration, the direction of the force parallel to the three sides of the fundamental cell, we generate three times as many data as the number of configurations. We write $\boldsymbol{V}$ as

$$\begin{aligned}\boldsymbol{V}(\boldsymbol{x}) \;&=\; [V]_F^0 \boldsymbol{W}_F \\ &\quad +\epsilon \sin(\boldsymbol{k}\cdot\boldsymbol{x}) \left([V]_F^{\parallel} \boldsymbol{W}_F^{\parallel} + [V]_F^{\perp} \boldsymbol{W}_F^{\perp} \right), \end{aligned} \tag{34}$$

and calculate the numerical coefficients $[V]_F^0$, $[V]_F^{\parallel}$, and $\boldsymbol{W}_F^{\parallel}$ by taking the ensemble average of the multipole coefficients appearing in the general expression (A1). We also have

$$\begin{aligned}\boldsymbol{u}_\Delta(\boldsymbol{x}) \;&=\; [u_\Delta]_F^0 \, \boldsymbol{W}_F \\ &\quad +\; \epsilon \sin(\boldsymbol{k}\cdot\boldsymbol{x}) \left([u_\Delta]_F^{\parallel} \, \boldsymbol{W}_F^{\parallel} + [u_\Delta]_F^{\perp} \, \boldsymbol{W}_F^{\perp} \right) \end{aligned} \tag{35}$$

with an expression for $\boldsymbol{u}_m$ similar to (17). Upon substitution of these parameterizations into the closure relation (32) and dropping some higher-order terms in k which do not contribute to the final result, we have

$$[V]_F^0 \;=\; V_1 [u_\Delta]_F^0, \tag{36}$$

$$[V]_F^{\parallel} \;=\; V_1 [u_\Delta]_F^{\parallel} + \phi \frac{\mathrm{d}V_1}{\mathrm{d}\phi} [u_\Delta]_F^0, \tag{37}$$

$$[V]_F^{\perp} \;=\; V_1 [u_\Delta]_F^{\perp} + \phi \frac{\mathrm{d}V_1}{\mathrm{d}\phi} [u_\Delta]_F^0 - V_3 (ka)^2 [u_m]_F^{\perp}, \tag{38}$$

The k-fits are now given by

$$[V]_F^0 \;=\; A^{[V]_F^0}, \tag{39}$$

$$[V]_F^{\parallel} \;=\; A^{[V]_F^{\parallel}} + kB^{[V]_F^{\parallel}} + k^2 C^{[V]_F^{\parallel}}, \tag{40}$$

$$[V]_F^{\perp} \;=\; A^{[V]_F^{\perp}} + kB^{[V]_F^{\perp}} + k^2 C^{[V]_F^{\perp}}, . \tag{41}$$

$$[u_\Delta]_F^0 \;=\; A^{[u_\Delta]_F^0} + (ka) B^{[u_\Delta]_F^0}, \tag{42}$$

$$[u_\Delta]_F^{\parallel} \;=\; A^{[u_\Delta]_F^{\parallel}} + (ka) B^{[u_\Delta]_F^{\parallel}}, \tag{43}$$

$$[u_\Delta]_F^{\perp} \;=\; A^{[u_\Delta]_F^{\perp}} + (ka) B^{[u_\Delta]_F^{\perp}}. \tag{44}$$

The coefficient V_1 of the uniform part is determined from (36) as

$$V_1 = \frac{A^{[V]_F^0}}{A^{[u_\Delta]_F^0}}. \tag{45}$$

Figure 4 shows this coefficient calculated from (45) divided by ϕ. It is seen that V_1 increases rapidly with concentration, which makes the effect of the corresponding term significant for non-dilute suspensions. These results can be fitted by

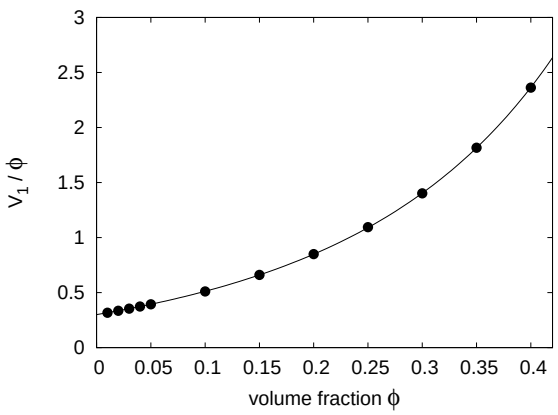

FIG. 4: The coefficient V_1 introduced in Eq. (32) and calculated from (45) divided by ϕ vs. volume fraction ϕ. The solid line corresponds to the fitting (46).

$$V_1(\phi) \;=\; \frac{3}{10}\phi + A \frac{\phi^2}{(1-\phi)^B}, \tag{46}$$

where the first term reproduces the dilute-limit result (9) and $A = 1.68$, $B = 2.20$.

From Eq. (37) we deduce, in the limit $k \to 0$,

$$\phi \frac{\mathrm{d}V_1}{\mathrm{d}\phi} = \frac{1}{A^{[u_\Delta]_F^0}} \left(A^{[V]_F^{\parallel}} - V_1 A^{[u_\Delta]_F^{\parallel}} \right), \tag{47}$$

in which the left-hand side arises similarly to (26). This relation affords an opportunity to check the robustness of the result for V_1. Figure 5 shows $\mathrm{d}V_1/\mathrm{d}\phi$ calculated from (47), as well as the estimation by numerical differentiation of (45) and analytical differentiation of the fit (46): all three results are consistent.

From Eq. (38), we have V_3 as

$$V_3 = -\frac{1}{D^{[u_m]_F^{\perp}}} \left(A^{[V]_F^{\perp}} - V_1 A^{[u_\Delta]_F^{\perp}} - \phi \frac{\mathrm{d}V_1}{\mathrm{d}\phi} A^{[u_\Delta]_F^0} \right). \tag{48}$$

The possibility of testing the consistency of V_3, and also of V_1, is offered by a consideration of the shear problem: from (A29) of the Appendix, we find

$$V_3 = -\frac{1}{D^{[u_m]_E^{\perp}}} \left(A^{[V]_E^{\perp}} - V_1 A^{[u_\Delta]_E^{\perp}} - V_2 \phi \right), \tag{49}$$

where the symbols have their usual meaning and V_2 is given by (A28):

$$V_2 = \frac{1}{\phi} \left(A^{[V]_E^{\parallel}} - V_1 A^{[u_\Delta]_E^{\parallel}} \right), \tag{50}$$

Figure 6 shows V_3/ϕ calculated from (48) and (49) with V_1 given by (45). Division by ϕ is suggested by the dilute-limit result (9) which predicts a value -11/140 for this quantity (horizontal line) as $\phi \to 0$, in good agreement

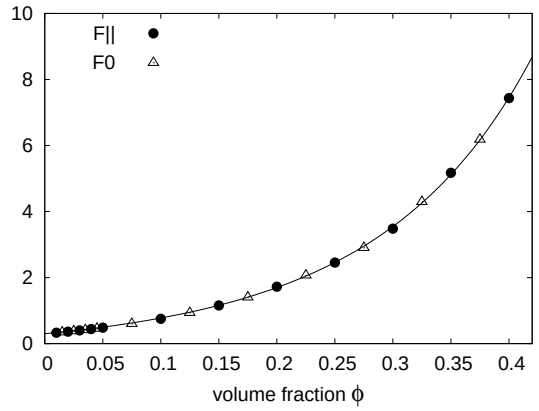

FIG. 5: Derivative $\mathrm{d}V_1/\mathrm{d}\phi$ of the coefficient V_1 from (47) (circles) compared with the numerical differentiation of the results of the previous figure (triangles). The solid line corresponds to the derivative calculated by the fitting (46).

with the numerical results. The slanted line represents the following fit:

$$V_3 = -\frac{11}{140}\phi + A\phi^2, \tag{51}$$

where $A = -0.313$. The consistency between the two determinations of V_3 is good in spite of some fluctuations amplified by the division by ϕ. This result also implies that V_1 calculated for the force problem gives a consistent result when used in expressions derived for the shear problem. This is an important conclusion irrespective of the actual importance of the terms of (32) beyond the first one.

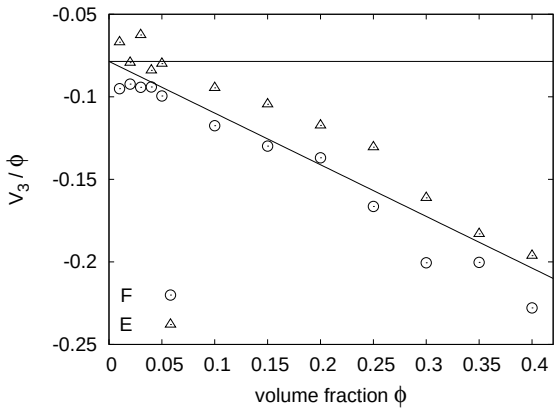

FIG. 6: Graph of V_3/ϕ obtained by (48) (circles) and (49) (triangles) compared with the dilute-limit result -11/140 shown by the horizontal line and the fitting (51).

Figure 7 shows V_2 calculated from (50). The horizontal line is the value 1/7 given by the dilute expression (9), with which the numerical results are in close agreement. For volume fractions of 30% and higher, the error is larger and it is difficult to make definite statements on the ϕ-dependence of this quantity in this range.

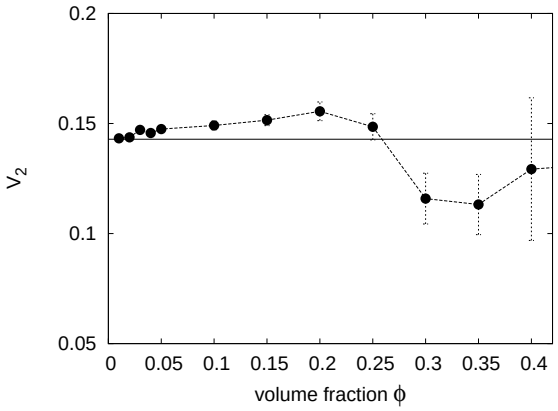

FIG. 7: The coefficient V_2; the solid line is the dilute-limit result 1/7.

For the coefficients V_4 and V_5 we can only generate a single relation from the torque problem (Eq. A27 in the Appendix), which is

$$\phi\left(V_4\frac{\mathrm{d}\Omega(\phi)}{\mathrm{d}\phi} + V_5\Omega(\phi)\right) = A^{[V]^{\perp}_T} - V_1 A^{[u_\Delta]^{\perp}_T} + V_3 D^{[u_m]^{\perp}_T}. \tag{52}$$

Here we use the results[30]

$$A^{[\Omega_\Delta]^0_T} = \Omega(\phi), \quad A^{[\Omega_\Delta]^{\perp}_T} = \phi\frac{\mathrm{d}\Omega(\phi)}{\mathrm{d}\phi}, \tag{53}$$

in which $\Omega(\phi)$ is the hindrance function for rotation in a uniform suspension defined by

$$\Omega(\phi)\frac{\boldsymbol{T}_0}{8\pi\mu a^3} = \boldsymbol{\Omega}_\Delta, \tag{54}$$

in which $\boldsymbol{T}_0$ is the couple acting on each particle. Our numerical results for this quantity[30] can be fitted by

$$\Omega = 1.0 - 1.5\phi + 0.67\phi^2 \tag{55}$$

Since we only have one equation for the two coefficients V_4 and V_5, we are unable to determine them independently. Their linear combination with the known function $\Omega(\phi)$ appearing in the left-hand side of Eq. (52) is proportional to ϕ^2 in the dilute limit, and is well fitted by

$$\phi\left(V_4\frac{\mathrm{d}\Omega(\phi)}{\mathrm{d}\phi} + V_5\Omega(\phi)\right) = \phi^2\left(A + \phi B\right), \tag{56}$$

where $A = -0.193$ and $B = -0.707$. Figure 8 shows theright-hand side of Eq. (52) divided by ϕ^2 as a function of ϕ, where the two earlier estimates (48) and (49) of V_3 are used.

The computed values of the coefficients of the vector $\boldsymbol{V}$ are shown in Table III.

In closing, it may be noted that the contribution of $\boldsymbol{V}$ to the momentum equation in the i-direction may be

TABLE III: Closure coefficients for $\boldsymbol{V}$.

ϕ	V_1	V_2	V_3		$\phi(V_4\Omega' + V_5\Omega)$	
			F	E	F	E
0.01	0.00312	0.143	−0.001	−0.0006	−0.00003	−0.00002
0.02	0.00654	0.14	−0.002	−0.0017	−0.00008	−0.00008
0.03	0.0103	0.15	−0.003	−0.0018	−0.0003	−0.0001
0.04	0.0144	0.15	−0.004	−0.003	−0.0003	−0.0003
0.05	0.0190	0.15	−0.006	−0.004	−0.0007	−0.0005
0.10	0.0489	0.15	−0.012	−0.009	−0.0029	−0.0023
0.15	0.095	0.15	−0.019	−0.016	−0.0070	−0.0058
0.20	0.166	0.16	−0.025	−0.024	−0.012	−0.011
0.25	0.269	0.15	−0.041	−0.033	−0.024	−0.021
0.30	0.41	0.11	−0.06	−0.05	−0.04	−0.04
0.35	0.63	0.10	−0.07	−0.07	−0.05	−0.05
0.40	0.94	0.2	−0.09	−0.08	−0.08	−0.08

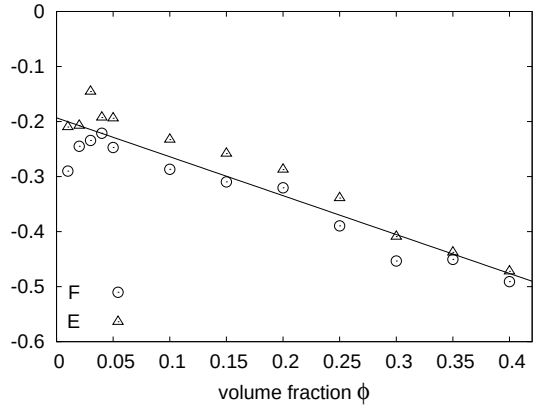

FIG. 8: $(V_4\Omega' + V_5\Omega)/\phi$ vs. ϕ obtained by (52) with V_3 of (48) (circles) and (49) (triangles).

written identically as

$$-(\boldsymbol{\nabla}\times\boldsymbol{\nabla}\times\boldsymbol{V})_i = \partial_j\left\{\left[\frac{1}{2}(\partial_j V_i + \partial_i V_j) - \frac{1}{3}\delta_{ij}\boldsymbol{\nabla}\cdot\boldsymbol{V}\right] + \frac{1}{2}(\partial_j V_i - \partial_i V_j) - \frac{2}{3}\delta_{ij}\boldsymbol{\nabla}\cdot\boldsymbol{V}\right\} \quad (57)$$

in which one recognizes a traceless symmetric term, an antisymmetric term, and an isotropic term. This was the decomposition of the stress adopted in Ref. 28, a study that was carried out before the form (1) of the stress was developed in Ref. 33.

V. THE AXIAL VECTOR OF THE ANTISYMMETRIC STRESS

In principle, the closure relation for the axial vector of the antisymmetric stress $\boldsymbol{R}$ may contain several terms,[28]

$$\begin{aligned}\boldsymbol{R} &= R_1\boldsymbol{\Omega}_\Delta \\ &\quad + R_2 a^2\boldsymbol{\nabla}\times(\mathsf{E}_m\cdot\boldsymbol{\nabla}\phi) + R_3 a^2\nabla^2\boldsymbol{\nabla}\times\boldsymbol{u}_m \\ &\quad + R_4 a^2\boldsymbol{\nabla}\times\boldsymbol{u}_\Delta + R_5(\boldsymbol{\nabla}\phi)\times\boldsymbol{u}_\Delta + \ldots. \end{aligned} \quad (58)$$

In this case, we discuss the parameterizations with reference to the torque problem (index T), which is characterized by the axial vector

$$\boldsymbol{\omega}_T = \frac{\boldsymbol{T}_0}{8\pi\mu a^3}, \quad (59)$$

which is the rotation velocity of a single isolated particle subjected to the couple $\boldsymbol{T}_0$; in this case there is only one polar vector characteristic of the problem, namely

$$\boldsymbol{W}_T^\perp = a\boldsymbol{k}\times\boldsymbol{\omega}_T. \quad (60)$$

By choosing, for each configuration, the direction of the torque parallel to the three sides of the fundamental cell, we effectively multiply by 3 the number of configurations used in the averaging as before.

We have

$$\begin{aligned}\boldsymbol{R}(\boldsymbol{x}) &= [R]_T^0\boldsymbol{\omega}_T \\ &\quad + \epsilon\sin(\boldsymbol{k}\cdot\boldsymbol{x})\left([R]_T^\parallel\boldsymbol{\omega}_T^\parallel + [R]_T^\perp\boldsymbol{\omega}_T^\perp\right), \end{aligned} \quad (61)$$

$$\boldsymbol{\Omega}_\Delta(\boldsymbol{x}) = [\Omega]_T^0\boldsymbol{\omega}_T + \epsilon\sin(\boldsymbol{k}\cdot\boldsymbol{x})\left([\Omega]_T^\parallel\boldsymbol{\omega}_T^\parallel + [\Omega]_T^\perp\boldsymbol{\omega}_T^\perp\right),$$

in which $\boldsymbol{\omega}_T^\parallel$ and $\boldsymbol{\omega}_T^\perp$ are the components of $\boldsymbol{\omega}_T$ parallel and perpendicular to $\boldsymbol{k}$.

From the closure relation (58) we deduce

$$[R]_T^0 = R_1[\Omega_\Delta]_T^0, \quad (62)$$

$$[R]_T^\parallel = R_1[\Omega_\Delta]_T^\parallel + \phi\frac{\mathrm{d}R_1}{\mathrm{d}\phi}[\Omega_\Delta]_T^0, \quad (63)$$

$$[R]_T^\perp = R_1[\Omega_\Delta]_T^\perp + \phi\frac{\mathrm{d}R_1}{\mathrm{d}\phi}[\Omega_\Delta]_T^0. \quad (64)$$

The k-dependent fits for the coefficients of $\boldsymbol{R}$ are

$$[R]_T^0 = A^{[R]_T^0}, \quad (65)$$

$$[R]_T^\parallel = A^{[R]_T^\parallel} + k^2 C^{[R]_T^\parallel}, \quad (66)$$

$$[R]_T^\perp = A^{[R]_T^\perp} + k^2 C^{[R]_T^\perp}, \quad (67)$$

$$[\Omega_\Delta]^0_T = A^{[\Omega_\Delta]^0_T}, \quad (68)$$

$$[\Omega_\Delta]^{\parallel}_T = A^{[\Omega_\Delta]^{\parallel}_T} + (ka)^2 C^{[\Omega_\Delta]^{\parallel}_T}, \quad (69)$$

$$[\Omega_\Delta]^{\perp}_T = A^{[\Omega_\Delta]^{\perp}_T} + (ka)^2 C^{[\Omega_\Delta]^{\perp}_T}. \quad (70)$$

From (62), which derives from the constant term of the torque problem, we have

$$R_1(\phi) = \frac{A^{[R]^0_T}}{A^{[\Omega_\Delta]^0_T}} = \frac{3\phi}{\Omega(\phi)}, \quad (71)$$

where use has been made of the fact that $A^{[R]^0_T}$ equals 3ϕ as shown in Ref. 28 and $A^{[\Omega_\Delta]^0_T}$ is $\Omega(\phi)$ as shown in (53). This result is consistent with the analysis of Batchelor[13] who showed that, for a uniform suspension, $\mu\boldsymbol{R} = \frac{1}{2}n_0\boldsymbol{T}_0$. In view of this relation, we give in Table IV, the numerical values of the hindrance function $\Omega(\phi)$, rather than of R_1.

When R_1 calculated from (71) is substituted into (63) ($T^{\parallel}$ term), we have

$$\phi\frac{\mathrm{d}R_1}{\mathrm{d}\phi} = \frac{1}{A^{[\Omega_\Delta]^0_T}}\left(A^{[R]^{\parallel}_T} - R_1 A^{[\Omega_\Delta]^{\parallel}_T}\right), \quad (72)$$

and in a similar way, from (64) ($T^{\perp}$ term),

$$\phi\frac{\mathrm{d}R_1}{\mathrm{d}\phi} = \frac{1}{A^{[\Omega_\Delta]^0_T}}\left(A^{[R]^{\perp}_T} - R_1 A^{[\Omega_\Delta]^{\perp}_T}\right). \quad (73)$$

Figure 9 shows $\mathrm{d}R_1/\mathrm{d}\phi$ calculated from (72) and (73)

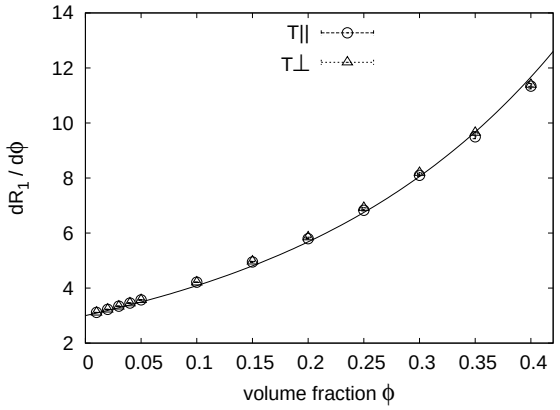

FIG. 9: $dR_1/d\phi$ from (72) (circles) and (73) (triangles); the line is the analytical derivative of a fit to the data.

as well as the derivative of R_1 calculated with the fit of Ω in (55). The consistency is very good which, once again, enables us to conclude that R_1 is a robust quantity independent of the specific flow. Furthermore, the simultaneous validity of (72) and (73) implies that, in a non-uniform system, R_1 and, therefore, $\Omega(\phi)$ can be evaluated using the local value of the volume fraction.

The fact that there are fewer axial than polar characteristic vectors reduces the number of relations that can be generated and therefore prevents us from determining more of the coefficients appearing in the closure relation (58).

TABLE IV: Hindrance function for rotation $\Omega(\phi)$.

ϕ	$\Omega(\phi)$
0.01	0.9853
0.02	0.9708
0.03	0.9563
0.04	0.9420
0.05	0.9278
0.10	0.8587
0.15	0.7923
0.20	0.7292
0.25	0.6689
0.30	0.6120
0.35	0.5579
0.40	0.5067

VI. SUMMARY AND CONCLUSIONS

Our study of the stress in a spatially non-uniform suspension of equal spheres in Stokes flow has been based on the identification of the three components of this quantity shown in Eq. (1): a symmetric traceless term, and an antisymmetric term consisting of an axial and a polar contribution. This result, derived in Ref. 33 and, more generally, in Ref. 37, extends the well-known work of Batchelor[13] to the non-homogeneous case. While the expressions derived in the references cited were general, the focus of this paper has been on the derivation of specific closure relations for these quantities.

The principal results of this work are the following:

1. By considering three different physical problems: particles subjected to a force, a torque, and shear, we found four independent determinations of the effective viscosity μ_e, all of which were shown to be numerically consistent. In the past, μ_e had been calculated only from the numerical simulation of the shearing of uniform suspensions. Our results imply that the same parameter can describe the stress in a suspension in different flow situations as well and is, therefore, a physically well-defined quantity having a meaning analogous to that of the ordinary viscosity in a Newtonian fluid.

2. The polar component of the antisymmetric stress, $\boldsymbol{V}$, is a new effect which had been identified before but for which no expression had been established. We have found a closure relation for this quantity, the coefficients of which also exhibit consistency among the different problems. Thus, the existence of this quantity appears to be well defined beyond any uncertainty deriving from statistical error. Furthermore, while some terms in the closure relation for $\boldsymbol{V}$ vanish as the particle radius is made smaller and smaller for a fixed volume fraction, the leading term does not. In principle, this contribution to the antisymmetric stress is therefore on the same footing as that of the effective viscosity.

3. We have also found consistency for the leading closure coefficient for the axial component $\boldsymbol{R}$ of the antisymmetric stress, which is related to the hindrance function for particle rotation.

4. We have determined that, to leading order in the spatial inhomogeneity, it is consistent to evaluate the closure coefficients of the leading terms in correspondence of the local volume fraction.

5. The fact that we have found an excellent consistency among the various determinations of the closure parameters suggests – although, of course, it does not prove – that the closures that we propose may be applicable to general flows beyond those that we have studied.

Due to the imperfectly understood consequences of the artificial periodicity arising from the use of a repeated fundamental cell, we have only been able to focus on the leading-order behavior in the wave number k of the spatial non-uniformity. To this order, we have found that the dominant term of the symmetric stress is the product of the effective viscosity and E_m, the rate of strain of the volumetric flux of the mixture $\boldsymbol{u}_m$. In comparison with this term, the other terms that could possibly be present give contributions lower by an order k^2, which our methods prevent us from determining.

Our results have been obtained by carrying out ensemble averages using biased probability distributions corresponding to a prescribed form of the particle number density. We have not attempted to incorporate any special structure for the two-particle and higher-order particle distribution functions which, as is well known, in general depend on the particular flow considered. In a recent paper,[30] we have shown how to bias the probability distribution so as to reproduce an arbitrary functional form for the particle number density. We believe that a similar approach may enable us to control the second- and higher-order distribution functions.

Acknowledgments

The numerical simulations were carried out with a code based on one kindly given to us by Prof. Sangani.

Support under DOE grant DE-FG02-99ER14966 is gratefully acknowledged.

APPENDIX A: DETAILS OF THE CLOSURES

1. Expression for the stress

Equation (1) was given as Eq. (10.19) in Ref. 33. General expressions for the various contributions were derived in terms of the coefficients appearing in Lamb's general solution of the Stokes equations[34–36] in the form

$$\mathsf{S} = \frac{4}{3}\pi\mu\sum_{l=2}^{\infty}\frac{(-1)^{l+1}}{l!}(2l+1)\mathcal{S}_l(a^2\nabla^2)\;\boldsymbol{\nabla}^{l-2}\cdot\left(n\overline{[\boldsymbol{\nabla}^l\,(r^{2l+1}q_{-l-1})]_{r=a}}\right), \tag{A1}$$

$$\boldsymbol{R} = \frac{4}{3}\pi\mu\sum_{l=2}^{\infty}\frac{(-1)^{l+1}}{(l-1)!}\left\{(2l+1)\mathcal{S}_l(a^2\nabla^2)\;\boldsymbol{\nabla}^{l-1}\cdot\left(n\overline{[\boldsymbol{\nabla}^l\,(r^{2l+1}\chi_{-l-1})]_{r=a}}\right)\right\}, \tag{A2}$$

$$\begin{aligned}\boldsymbol{V} = \frac{4}{3}\pi\mu\sum_{l=2}^{\infty}\frac{(-1)^{l+1}}{l!}\Big\{&(2l+1)(2l+3)\mathcal{S}_{l+1}(a^2\nabla^2)\;\boldsymbol{\nabla}^{l-1}\cdot\left(n\overline{\left[\boldsymbol{\nabla}^l\left(r^{2l+1}\phi^*_{-l-1}\right)\right]_{r=a}}\right)\\ &+a^2\mathcal{S}_{l+1}(a^2\nabla^2)\;\boldsymbol{\nabla}^{l-1}\cdot\left(n\overline{[\boldsymbol{\nabla}^l\,(r^{2l+1}q_{-l-1})]_{r=a}}\right)\Big\}.\end{aligned} \tag{A3}$$

Here the operators $\mathcal{S}_l$ are defined by

$$\mathcal{S}_l = \frac{3}{(2l+1)!!}\left[1+\frac{a^2\nabla^2}{1!2^1(2l+3)}+\frac{(a^2\nabla^2)^2}{2!2^2(2l+3)(2l+5)}+\ldots\right]. \tag{A4}$$

The term $\left[\boldsymbol{\nabla}^l\left(r^{2l+1}q_{-l-1}\right)\right]_{r=a}$ and similar ones are constants, and the overline denotes the ensemble average.

2. The symmetric part of the stress S

An expanded form of the closure relation (10) for the symmetric part of the stress S by $\boldsymbol{u}_m$, $\boldsymbol{u}_\Delta$, $\boldsymbol{\Omega}_\Delta$, and ϕ is

$$\begin{aligned}2\mathsf{E}_m+\mathsf{S} = {}& 2\mu_e\mathsf{E}_m+2\mu_\Delta\mathsf{E}_\Delta+2\mu_\nabla\mathsf{E}_\nabla+2\mu_\Omega\mathsf{E}_\Omega\\ &+2\mu_0a^2\nabla^2\mathsf{E}_m+2\mu_1a^2\mathsf{E}_m\nabla^2\phi+\ldots\end{aligned} \tag{A5}$$

where E_Δ, E_∇, and E_Ω, are defined by

$$\mathsf{E}_\Delta = \frac{1}{2}\left[\boldsymbol{\nabla u}_\Delta + (\boldsymbol{\nabla u}_\Delta)^\dagger\right] - \frac{1}{3}(\boldsymbol{\nabla}\cdot\boldsymbol{u}_\Delta)\,\mathsf{I}, \quad \text{(A6)}$$

$$\mathsf{E}_\nabla = \frac{1}{2}\left[\boldsymbol{u}_\Delta\boldsymbol{\nabla}\phi + (\boldsymbol{u}_\Delta\boldsymbol{\nabla}\phi)^\dagger\right] - \frac{1}{3}(\boldsymbol{u}_\Delta\cdot\boldsymbol{\nabla}\phi)\,\mathsf{I}, \quad \text{(A7)}$$

$$\mathsf{E}_\Omega = \frac{1}{2}\left[\{\boldsymbol{\nabla}(\boldsymbol{\nabla}\times\boldsymbol{\Omega}_\Delta)\} + \{\boldsymbol{\nabla}(\boldsymbol{\nabla}\times\boldsymbol{\Omega}_\Delta)\}^\dagger\right]. \quad \text{(A8)}$$

In Sec. III, the shear problem is discussed in detail. Here we summarize the parameterizations and k-dependencies for the force and torque problems. For the former:

$$\mathsf{S}(\boldsymbol{x}) = \epsilon\cos(\boldsymbol{k}\cdot\boldsymbol{x})\left([S]^\perp_F\mathsf{G}^\perp_F + [S]^\parallel_F\mathsf{G}^\parallel_F\right), \quad \text{(A9)}$$

and for the latter:

$$\mathsf{S}(\boldsymbol{x}) = \epsilon\sin(\boldsymbol{k}\cdot\boldsymbol{x})\,[S]^\perp_T\mathsf{G}^\perp_T. \quad \text{(A10)}$$

The coefficients are fitted as

$$[S]^\parallel_F = \frac{1}{k}\left(0 + k^2A^{[S]^\parallel_F} + k^3B^{[S]^\parallel_F}\right), \quad \text{(A11)}$$

$$[S]^\perp_F = \frac{1}{k}\left(D^{[S]^\perp_F} + k^2A^{[S]^\perp_F} + k^3B^{[S]^\perp_F}\right), \quad \text{(A12)}$$

$$[S]^\perp_T = D^{[S]^\perp_T} + k^2A^{[S]^\perp_T}. \quad \text{(A13)}$$

Upon substituting the parameterizations into the closure relation (A5), we find the seven relations

$$[S]^0_E = 2\mu_e \quad \text{(A14)}$$

$$[S]^E_E = 2\phi\left(1-\frac{k^2}{10}\right)\left(\frac{\mathrm{d}\mu_e}{\mathrm{d}\phi} - k^2\mu_1\right), \quad \text{(A15)}$$

$$\frac{[S]^\parallel_E}{2} = -\mu_\Delta k[u_\Delta]^\parallel_E, \quad \text{(A16)}$$

$$[S]^\perp_E = -\left(\mu_e - k^2\mu_0\right)k[u_m]^\perp_E - \mu_\Delta k[u_\Delta]^\perp_E + \mu_\Omega k^2[\Omega_\Delta]^\perp_E \quad \text{(A17)}$$

$$[S]^\perp_T = -\left(\mu_e - k^2\mu_0\right)k[u_m]^\perp_T - \mu_\Delta k[u_\Delta]^\perp_T - \mu_\Omega k^2[\Omega_\Delta]^\perp_T, \quad \text{(A18)}$$

$$\frac{[S]^\parallel_F}{2} = \mu_\Delta k[u_\Delta]^\parallel_F + \mu_\nabla\phi\left(1-\frac{k^2}{10}\right)k[u_\Delta]^0_F, \quad \text{(A19)}$$

$$[S]^\perp_F = \left(\mu_e - k^2\mu_0\right)k[u_m]^\perp_F + \mu_\Delta k[u_\Delta]^\perp_F + \mu_\nabla\phi\left(1-\frac{k^2}{10}\right)k[u_\Delta]^0_F + \mu_\Omega k^2[\Omega_\Delta]^\perp_F. \quad \text{(A20)}$$

By considering the k-dependencies of the averages of $[S]$, $[u_m]$, $[u_\Delta]$, and $[\Omega_\Delta]$, up to $O(k^0)$, we have only the terms with μ_e exhibited in the text.**?

3. The polar vector of the antisymmetric stress $\boldsymbol{V}$

In Sec. IV, the parameterization of the polar vector of the antisymmetric stress $\boldsymbol{V}$ for the force problem is given by (34). The parameterizations for the torque and shear problems are

$$\boldsymbol{V}(\boldsymbol{x}) = \epsilon\cos(\boldsymbol{k}\cdot\boldsymbol{x})\,[V]^\perp_T\boldsymbol{W}^\perp_T, \quad \text{(A21)}$$

and

$$\boldsymbol{V}(\boldsymbol{x}) = \epsilon\cos(\boldsymbol{k}\cdot\boldsymbol{x})\left([V]^\parallel_E\boldsymbol{W}^\parallel_E + [V]^\perp_E\boldsymbol{W}^\perp_E\right), \quad \text{(A22)}$$

respectively.

The k-fits of the $[V]$'s for the torque and shear problems are

$$[V]^\perp_T = k\left(A^{[V]^\perp_T} + kB^{[V]^\perp_T}\right), \quad \text{(A23)}$$

$$[V]^\parallel_E = k\left(A^{[V]^\parallel_E} + kB^{[V]^\parallel_E}\right), \quad \text{(A24)}$$

$$[V]^\perp_E = k\left(A^{[V]^\perp_E} + kB^{[V]^\perp_E}\right). \quad \text{(A25)}$$

Upon substituting these parameterizations and the corresponding ones for the velocities into the closure relation (32) and equating the corresponding terms, we find Eqs. (36) and (37) in the text and

$$[V]^\perp_F = V_1[u_\Delta]^\perp_F + \phi\frac{\mathrm{d}V_1}{\mathrm{d}\phi}[u_\Delta]^0_F - V_3k^2[u_m]^\perp_F + V_4k[\Omega_\Delta]^\perp_F, \quad \text{(A26)}$$

$$[V]^\perp_T = V_1[u_\Delta]^\perp_T - V_3(ka)^2[u_m]^\perp_T + V_4k[\Omega_\Delta]^\perp_T + V_5k\phi[\Omega_\Delta]^0_T, \quad \text{(A27)}$$

$$[V]^\parallel_E = V_1[u_\Delta]^\parallel_E + V_2ka\phi, \quad \text{(A28)}$$

$$[V]^\perp_E = V_1[u_\Delta]^\perp_E - V_3k^2[u_m]^\perp_E + V_2k\phi - V_4k[\Omega_\Delta]^\perp_E. \quad \text{(A29)}$$

Dropping the terms with $O(k^2)$ in (A26), we only show the leading terms in (38) in the text.

4. The axial vector of the antisymmetric stress $\boldsymbol{R}$

For the force problem, the axial vector of the antisymmetric stress $\boldsymbol{R}$ is parameterized as

$$\boldsymbol{R}(\boldsymbol{x}) = \epsilon\cos(\boldsymbol{k}\cdot\boldsymbol{x})\,[R]^\perp_F\boldsymbol{\omega}^\perp_F, \quad \text{(A30)}$$

and for the shear problems as

$$\boldsymbol{R}(\boldsymbol{x}) = \epsilon\sin(\boldsymbol{k}\cdot\boldsymbol{x})\,[R]^\perp_E\boldsymbol{\omega}^\perp_E, \quad \text{(A31)}$$

in which $\boldsymbol{\omega}^\perp$ is the component of the characteristic axial vector $\boldsymbol{\omega}_T$ ** perpendicular to $\boldsymbol{k}$.

The k-dependent fits for the coefficients of $\boldsymbol{R}$ for the force and shear problems are

$$[R]^\perp_F = k\left(A^{[R]^\perp_F} + kB^{[R]^\perp_F}\right), \quad \text{(A32)}$$

$$[R]^\perp_E = k^2\left(A^{[R]^\perp_E} + kB^{[R]^\perp_E}\right). \quad \text{(A33)}$$

As before, substituting these parameterizations and k-fittings into the closure relation (58), we find Eqs. (62) and (63), and

$$
\begin{aligned}
[R]^{\perp}_{T} &= R_1[\Omega_\Delta]^{\perp}_{T} + \phi\frac{\mathrm{d}R_1}{\mathrm{d}\phi}[\Omega_\Delta]^{0}_{T} \\
&\quad + R_3 k^3 [u_m]^{\perp}_{T} - R_4 k [u_\Delta]^{\perp}_{T}, \qquad \text{(A34)} \\
[R]^{\perp}_{F} &= R_1[\Omega_\Delta]^{\perp}_{F} \\
&\quad - R_3 k^3 [u_m]^{\perp}_{F} + R_4 k [u_\Delta]^{\perp}_{F} \\
&\quad + R_5 \phi k [u_\Delta]^{0}_{F}, \qquad \text{(A35)} \\
[R]^{\perp}_{E} &= -\frac{R_3}{2} k [u_m]^{\perp}_{E} + R_1[\Omega_\Delta]^{\perp}_{E} \\
&\quad + R_3 k^3 [u_m]^{\perp}_{E} - R_4 k [u_\Delta]^{\perp}_{E} \\
&\quad - R_2 k^2 \phi. \qquad \text{(A36)}
\end{aligned}
$$

Note that (A34) includes higher order terms in k which are neglected in (64) in the text. Even though we have five equations for the closure of $\boldsymbol{R}$, we cannot determine all the five coefficients appearing in the closure relation as the three equations for the torque problem essentially contain only R_1. Thus, we are left with only two equations to determine the four remaining coefficients.

* Electronic address: ichiki@mailaps.org
† Electronic address: prosperetti@jhu.edu

[1] M. Ishii, *Thermo-Fluid Dynamic Theory of Two-Phase Flow* (Eyrolles, Paris, 1975).
[2] D. A. Drew, "Mathematical modeling of two-phase flow," Ann. Rev. Fluid Mech. **15**, 261 (1983).
[3] D. D. Joseph and T. S. Lundgren, "Ensemble averaged and mixture theory equations for incompressible fluid-particle suspensions," Int. J. Multiphase Flow **16**, 35 (1990).
[4] A. Prosperetti, "Some considerations on the modeling of disperse multiphase flows by averaged equations," JSME Int. J. **B42**, 573 (2000).
[5] T. B. Anderson and R. Jackson, "A fluid mechanical description of fluidized beds," I & EC Fundamentals **6**, 527 (1967).
[6] S. Sundaresan, "Instabilities in fluidized beds," Ann. Rev. Fluid Mech. **35**, 63 (2003).
[7] D. L. Koch, "Kinetic theory for a monodisperse gas-solid suspension," Phys. Fluids **A2**, 1711 (1990).
[8] H. K. Tsao and D. L. Koch, "Simple shear flows of dilute gas-solid suspensions," J. Fluid Mech. **296**, 211 (1995).
[9] A. S. Sangani, G. B. Mo, H. K. Tsao, and D. L. Koch, "Simple shear flow of dense gas-solid suspensions at finite Stokes numbers," J. Fluid Mech. **313**, 309 (1996).
[10] S. Y. Kang, A. S. Sangani, H. K. Tsao, and D. L. Koch, "Rheology of dense bubble suspensions," Phys. Fluids **9**, 1540 (1997).
[11] D. L. Koch and A. S. Sangani, "Particle pressure and marginal stability limits for a homogeneous monodisperse gas-fluidized bed: kinetic theory and numerical simulations," J. Fluid Mech. **400**, 229 (1999).
[12] R. J. Phillips, R. C. Armstrong, and R. A. Brown, "A constitutive equation for concentrated suspensions that accounts for the shear-induced particle migration," Phys. Fluids **A4**, 30 (1992).
[13] G. K. Batchelor, "The stress system in a suspension of force-free particles," J. Fluid Mech. **41**, 545 (1970).
[14] J. F. Brady and J. F. Morris, "Microstructure of strongly sheared suspensions and its impact on rheology and diffusion," J. Fluid Mech. **348**, 103 (1997).
[15] J. Bergenholtz, J. F. Brady, and M. Vicic, "The non-Newtonian rheology of dilute colloidal suspensions," J. Fluid Mech. **456**, 239 (2002).
[16] J. F. Brady, "The rheological behavior of concentrated colloidal dispersions," J. Chem. Phys. **99**, 567 (1993).
[17] D. L. Koch and A. J. C. Ladd, "Moderate Reynolds number flow through periodic and random arrays of aligned cylinders," J. Fluid Mech. **349**, 31 (1997).
[18] N. A. Patankar, D. D. Joseph, J. Wang, R. D. Barree, M. Conway, and M. Asadi, "Power law correlations for sediment transport in pressure driven channel flows," Int. J. Multiphase Flow **28**, 1269 (2002).
[19] A. Biesheuvel and S. Spoelstra, "The added mass coefficient of a dispersion of spherical gas bubbles in liquid," Int. J. Multiphase Flow **15**, 911 (1989).
[20] A. S. Sangani and A. K. Didwania, "Dispersed-phase stress tensor in flows of bubbly liquids at large Reynolds numbers," J. Fluid Mech. **248**, 27 (1993).
[21] D. Z. Zhang and A. Prosperetti, "Averaged equations for inviscid disperse two-phase flow," J. Fluid Mech. **267**, 185 (1994).
[22] P. D. M. Spelt and A. S. Sangani, "Properties and averaged equations for flows of bubbly liquids," Appl. Sci. Res. **58**, 337 (1997/1998).
[23] J. F. Brady and G. Bossis, "Stokesian dynamics," Ann. Rev. Fluid Mech. **20**, 111 (1988).
[24] C. C. Chang and R. L. Powell, "The rheology of bimodal hard-sphere dispersions," Phys. Fluids **6**, 1628 (1994).
[25] C. K. Aidun, Y. Lu, and E.-J. Ding, "Direct analysis of particulate suspensions with inertia using the discrete Boltzmann equation," J. Fluid Mech. **37**, 287 (1998).
[26] M. Marchioro and A. Acrivos, "Shear-induced particle diffusivities from numerical simulations," J. Fluid Mech. **443**, 101 (2001).
[27] M. Marchioro, M. Tanksley, and A. Prosperetti, "Flow of spatially non-uniform suspensions. Part I: Phenomenology," Int. J. Multiphase Flow **26**, 783 (2000).
[28] M. Marchioro, M. Tanksley, W. Wang, and A. Prosperetti, "Flow of spatially non-uniform suspensions. Part II: Systematic derivation of closure relations," Int. J. Multiphase Flow **27**, 237 (2001).
[29] W. Wang and A. Prosperetti, "Flow of spatially non-uniform suspensions. Part III: Closure relations for porous media and spinning particles," Int. J. Multiphase Flow **27**,

1627 (2001).
[30] K. Ichiki and A. Prosperetti, "Faxén-like relations for a non-uniform suspension," Phys. Fluids **16**, 2483 (2004).
[31] Q. Zhang, K. Ichiki, and A. Prosperetti, "Ensemble averaging for spatially non-uniform systems," Phys. Rev. E. (submitted)
[32] R. A. Lionberger and W. B. Russel, "Microscopic theories of the rheology of stable colloidal dispersions," Adv. Chem. Phys. **111**, 399 (2000).
[33] M. Tanksley and A. Prosperetti, "Average pressure and velocity fields in non-uniform suspensions of spheres in Stokes flow," J. Eng. Math. **41**, 275 (2001).
[34] H. Lamb, *Hydrodynamics*, 6th ed. (Cambridge U.P., Cambridge, 1932).
[35] J. Happel and H. Brenner, *Low-Reynolds Number Hydrodynamics* (Prentice-Hall, Englewood Cliffs, 1965).
[36] S. Kim and S. J. Karrila, *Microhydrodynamics* (Butterworth-Heinemann, Boston, 1991).
[37] A. Prosperetti, "The average stress in incompressible disperse flow, *Int. J. Multiphase Flow*," Int. J. Multiphase Flow (2004). (submitted)
[38] L. D. Landau and E. M. Lifshitz, *Fluid Mechanics* (Pergamon, Oxford, 1959).
[39] C. W. J. Beenakker, "The effective viscosity of a concentrated suspension of spheres (and its relation to diffusion)," Physica **128A**, 48 (1984).
[40] D. R. Foss and J. F. Brady, "Structure, diffusion and rheology of Brownian suspensions by Stokesian Dynamics simulation," J. Fluid Mech. **407**, 167 (2000).
[41] G. K. Batchelor and J. T. Green, "The hydrodynamic interaction of two small freely-moving spheres in a linear flow field," J. Fluid Mech. **56**, 375 (1972).
[42] A. J. C. Ladd, "Hydrodynamic transport coefficients of random dispersions of hard spheres," J. Chem. Phys. **93**, 3484 (1990).
[43] K. C. Nunan and J. B. Keller, "Effective viscosity of a periodic suspension," J. Fluid Mech. **142**, 269 (1984).